Iraqi Journal of Science, 2025, Vol. 66, No. 11, pp: 5248- 5259
DOI: 10.24996/ijs.2025.66.11.43

ISSN: 0067-2904

Optical Emission Spectroscopic Technique for Diagnosis of Plasma Parameters of the Comet Tail

Waleed Ibrahim Yaseen*, Omar Al-Juboori, Khalid A. Hadi
Department of Astronomy and Space, College of Science, University of Baghdad, Baghdad, Iraq

Received: 11/7/2024 Accepted: 24/11/2024 Published: 30/11/2025

Abstract

In this work, the optical emission spectroscopy technique was employed to diagnose the plasma and solar wind parameters of Comet C/2020 F3 from July 21 to July 31, 2020. Datasets of comet C2020 F3 (NEOWISE) were gathered using the Cassegrain telescope camera CTK-II providing information within the visible spectrum, particularly emission lines within the wavelength range of 560 to 636 nanometers. The investigation utilized a two-line ratio method to scrutinize the spectrum of the comet over a five-day period from July 21 to July 31, 2020. Furthermore, various plasma parameters such as electron temperature, electron density, Debye length, and plasma frequency were determined. The study also delved into solar wind parameters that align with the comet plasma parameters, including solar wind temperature (in Kelvin), proton density (measured in $1/cm^3$), solar wind speed (in kilometers per second), and magnetic field strength (denoted as B_x, B_y, and B_z) in nT. The findings obtained from the analysis of the spectrum were employed to identify the chemical composition of the comet plasma. The results of this study are evident in a correlation between the intensity of these emissions and the distance of the comet from the Sun. It was observed that the heightened values of solar wind speed and temperature, particularly between the 25th and 28th of July, influenced the temperature and electron density of the plasma. During the 30^{th} and 31^{st} days of July, there was a decrease in both electron temperature and electron density as the comet moved farther away from the Sun.

Keywords: Optical emission spectroscopy, Boltzmann and Lorentz techniques, comets tails, plasma parameters.

التقنية الطيفية للانبعاث البصري لتشخيص معلمات البلازما في ذيل المذنب

وليد ابراهيم ياسين* ,عمر طارق علي , خالد عبد الكريم هادي
قسم الفلك والفضاء، كلية العلوم، جامعة بغداد، بغداد، العراق

الخلاصة

في هذا العمل، تم استخدام تقنية التحليل الطيفي للانبعاث البصري لتشخيص معاملات البلازما والرياح الشمسية للمذنب C/2020 F3 خلال الفترة من 21 يوليو إلى 31 يوليو 2020. تم جمع البيانات الخاصة بمذنب C/2020 F3 (NEOWISE) باستخدام كاميرا تلسكوب Cassegrain (CTK-II)، التي توفر المعلومات ضمن الطيف المرئي، وخاصة خطوط الانبعاث ضمن نطاق الطول الموجي من 560 إلى 636 نانومتر. استخدمت الدراسة طريقة النسبة ذات الخطين لفحص طيف المذنب على مدى خمسة أيام من 21

*Email: waleedib1972cnc@gmail.com

يوليو إلى 31 يوليو 2020. علاوة على ذلك، تم حساب معلمات البلازما المختلفة، مثل درجة حرارة الإلكترون، وكثافة الإلكترون، وطول ديباي، و تردد البلازما. كما تطرق البحث أيضاً لدراسة معاملات الرياح الشمسية التي تتوافق مع معلمات بلازما المذنب، بما في ذلك درجة حرارة الرياح الشمسية (كلفن)، وكثافة البروتون 1/سنتمتر مكعب، وسرعة الرياح الشمسية (كم/ثانية)، وقوة المجال المغناطيسي (B_x وB_y وB_z) (nT). تم استخدام النتائج المستمدة من تحليل الطيف لتحديد التركيب الكيميائي لبلازما المذنب.حيث كشفت نتائج هذه الدراسة عن وجود علاقة بين شدة هذه الانبعاثات وبعد المذنب عن الشمس. وقد لوحظ أن القيم المرتفعة لسرعة الرياح الشمسية ودرجة حرارتها، خاصة بين 25 و28 يوليو، من المحتمل أن تؤثر على درجة الحرارة وكثافة الإلكترونات في البلازما. خلال يومي 30 و31 من شهر يوليو، كان هناك انخفاض في كل من درجة حرارة الإلكترون وكثافة الإلكترونات مع تحرك المذنب بعيدًا عن الشمس.

1. Introduction

Comets are celestial objects that have amazed humanity for centuries with their spectacular appearances in the night sky. These icy bodies originate from the outer regions of our solar system, often referred to as the Oort Cloud and the Kuiper Belt. Comets consist of a nucleus made up of ice, dust, volatile gases, and organic compounds. As they approach the Sun during their orbits, they undergo a stunning transformation. Intense solar radiation causes the ice to sublime, releasing gases and dust that create a glowing coma around the nucleus. The pressure of sunlight and the solar wind push these materials away from the nucleus, forming iconic tails that can extend for millions of kilometers [1]. Comets have played a crucial role in our understanding of the solar system's formation and evolution as they preserve ancient materials from the early stages of its development. Studying comets provides insights into the composition of the early solar nebula and the conditions under which planets formed. The study of comets has also contributed to our understanding of the interplay between the solar wind and the interstellar medium [2]. The heated corona's base is where the solar wind begins, and it is propelled to supersonic speeds as it gets closer to the Sun. It continually blows, expanding the heliosphere. There are almost equal amounts of both electrons and ions in it. Protons comprise most of the ion components (95%), with a tiny quantity of doubly ionized helium and heavier ions. The density, speed, temperature, intensity, and direction of the flow's embedded magnetic field are all variable characteristics of the solar wind [3]. The solar wind affects the formation of the Earth's ionosphere [4]. Comet C/2020 F3, also known as NEOWISE, captivated the world's attention in 2020 as a spectacular celestial visitor. Discovered by NASA's Near-Earth Object Wide-field Infrared Survey Explorer (NEOWISE) mission on March 27, 2020, the comet gained widespread visibility during its close approach to the Sun. NEOWISE was characterized by its distinctive twin tails - a blue ion tail and a curved dust tail - which formed as volatile gases and dust were released from the comet's nucleus due to solar heating. The comet's brightness and prominent tails made it visible to the naked eye, providing a rare opportunity for skywatchers and astronomers alike to observe its beauty. (NASA's NEOWISE Mission Spots a Comet) [5]. The unique passage of this very bright comet offered a unique opportunity to deeply investigate the emission spectrum of a comet at high resolution. The study of their emission lines is a large source of information on the coma composition, the physical phenomena occurring in the coma, and the composition of the nucleus [6]. The complex molecular spectrum of the coma of a comet results in thousands of lines being visible in the spectral region from 3800–10200 A [7]. In this work, the study was conducted based on the result of an observational study of NEOWISE using the Nazionale Galileo (TNG) 3.6 m telescope [8].

2. Plasma Parameters

Plasma properties are important for understanding the complex behavior between the solar wind and the comet's coma and the dynamic behavior of these celestial bodies. Comets create

a plasma atmosphere around themselves as they get closer to the Sun because they emit ions and electrons from their nucleus. Important factors that describe the behavior of this cometary plasma include electron density, ion and electron temperatures, plasma frequency, and collision frequency. Recently, these factors have been studied in relation to comets. An example is the work by Tenishev [9], which focuses on electron density and temperature variations in the cometary coma, shedding light on the plasma dynamics. Additionally, the research by Richter [10] discusses the importance of ion temperature measurements in understanding the interaction between solar wind and cometary plasma. These contemporary references underscore the ongoing research efforts to characterize and interpret plasma parameters in the unique environment of comets, enhancing our understanding of their behavior and evolution. The plasma parameters include:

2.1Electron Temperature (T_e)

As free electrons are accountable for exciting atoms and molecules, the interrelation between electron temperature (T_e) and excitation temperature (T_{ext}) becomes significant. The emitted line intensity serves as a descriptor of plasma physical properties. When the local thermodynamic equilibrium (LTE) condition is satisfied for the upper energy levels of two lines, determining T_e becomes straightforward using the intensity ratio method [11]. By evaluating the intensity of individual hydrogen emission spectral lines within the Balmer region, the electron temperature is computed using the associated formula [12]:

$$T_e = \frac{\Delta E}{\ln\left[\frac{A_1 g_1 \lambda_2 I_2}{A_2 g_2 \lambda_1 I_1}\right] K} \quad (1)$$

Where: (ΔE, I, λ, g, K, and A) are the energy difference between two levels, intensity, wavelength, statistical weighting factor, Boltzmann constant, and transition probability, respectively.

2.2 Electron Density (n_e)

In situations where the plasma closely approaches conditions of local thermodynamic equilibrium (LTE), the electron density (n_e) can be determined by analyzing the intensity ratio of two lines associated with distinct ionization stages of a single element using the Saha Boltzmann method [13]. The calculation of electron density involves:

$$n_e = \frac{\lambda_1 I_1 / A_1 g_1}{\lambda_2 I_2 / A_2 g_2}\, 6.04x10^{21} T^{3/2} e^{\left[\frac{(-E_2+E_1-X_1)}{KT}\right]} \quad (2)$$

Where: (I_1 and I_2) are the net emission intensity of the ion and neutral lines, respectively; (g.A) is the product of the statistical weight and of the transition probability; (λ) is the wavelength in nm; (n_e) the electron density; (*X*) is the ionization temperature; and (E_1 and E_2) are the excitation energies of the ion and the atom, respectively [14].

2.3 Debye Length (λ_D)

Within plasma, electrons exhibit attraction towards adjacent ions, effectively screening their electrostatic fields from the surrounding plasma environment. Conversely, a stationary electron repels its counterparts while drawing in ions, thereby modifying the potential in the vicinity of a charged particle. If the plasma held an excess of either positive or negative particles, this surplus would generate an electric field compelling electrons to migrate and neutralize the charge. This phenomenon, termed Debye Shielding, prompts charged particles to counteract the influence of localized electric fields, a process that bestows upon plasma its characteristic quasi-neutrality. The resulting electric potential is primarily concentrated near

the particle's surface, spanning a distance known as the length of Debye (λ_D) which is defined by [15] [16]:

$$\lambda_D = \sqrt{\frac{\varepsilon_o K T_e}{e^2 n_e}} \quad (3)$$

Where: (λ_D) is the Debye length, (ε_o) is the space permittivity, (e) is the charge of the electron.

2.4 Plasma frequency (ω_p)

The plasma frequency stands as a noteworthy plasma parameter, setting it apart from the electron plasma frequency. This parameter signifies the characteristic frequency at which electrostatic oscillations occur due to the slight charge separation of electrons (e) within the plasma. This frequency can be calculated using the formula [17]:

$$\omega_p = \sqrt{\frac{n_e e^2}{\varepsilon_o m_e}} \quad (4)$$

3. Spectroscopic Observations

The Échelle spectrograph FLECHAS was utilized to observe Comet C/2020 F3 (NEOWISE) for five nights in late July 2020 [18]. It worked at the (*Nasmyth*) focus of the 90 cm telescope situated at the University Observatory Jena [19]. Throughout the observations, the spectrograph's fiber, with a diameter of 3.9 arcsec when projected onto the sky, was consistently directed toward the comet coma, as depicted in Figure 1 [20].

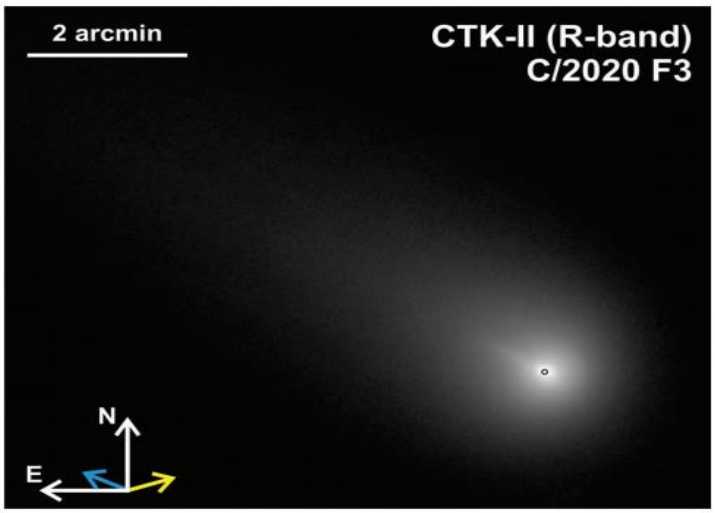

Figure 1: Image of Comet C/2020 F3 (NEWOWISE) [20].

The presented figure illustrates a comprehensive R-band image capturing the coma and initial segment of the tail of comet C/2020 F3 (NEOWISE). This image was acquired at 20:30 UT on July 23, 2020, signifying the observation's midpoint. The image was taken employing the Cassegrain Telescope camera CTK-II, which is in operation at the University Observatory Jena's 25 cm Cassegrain telescopes [21]. A comprehensive description of the instrument configuration utilized each night is provided in the observation log, which is outlined in Table 1. Additionally, a compilation of the Heliocentric Distance (r) of the comet and its Earth distance (Δ) for all observation sessions was listed in Table 1 [20].

Table 1: Observation Log [20].

Obs. mid time [Date UT]	r [au]	Δ [au]
21 July 2020	0.6040	0.6938
23 July 2020	0.6481	0.6928
29 July 2020	0.7813	0.7537
30 July 2020	0.8025	0.7710
31 July 2020	0.8241	0.7906

4. Solar Winds

Solar winds are a continuous plasma stream originating from the solar corona and extending into interplanetary space. Primarily composed of protons, electrons, and a limited number of heavier ions, solar winds radiate outwards in all directions [22]. Additionally, they demonstrate super-Alfvénic and supersonic characteristics near Earth's orbit. Typically, the solar wind's velocity is around 350 km/s at a distance of 1 Astronomical Unit (AU). Remarkably, it takes approximately four days for solar winds to traverse the distance from the Sun to Earth [23]. The Interplanetary Magnetic Field (IMF) serves as an indicator of the solar wind's magnetic field, which is intricately linked to the movement of solar wind plasma and is often described as being "frozenin" to the plasma movement. Moreover, solar winds can be categorized into two distinct types: slow and fast solar winds [24].

Solar wind parameters encompass a range of critical aspects that characterize the properties of the solar wind [25]. These parameters include Solar Wind Speed, Solar Wind, Temperature proton Density Proton Flux, Electric Field, Magnetic Field Strength, and Interplanetary Magnetic Field (IMF). These parameters collectively provide a comprehensive understanding of the solar wind properties and its interactions with the space environment [26].

5. Results and Discussion

Comet C/2020 F3 was observed by the Galileo National Telescope for the period from July 21 to 31, 2020. The collected data provided information on the visible spectrum which depicts the relationship between intensity and wavelength. Notably, the emission lines of comet C/2020 F3 were observed within the wavelength range of (560 to 636) nm. The spectrum illustrates the relation between intensity (measured in arbitrary units (a.u.)) and wavelength (measured in nanometers (nm)). The observed spectrum exhibits two distinct features, namely oxygen (O_2) and (NH_2). These features are characterized by emission lines with distinct peaks, as illustrated in Figure 2. Specifically, the emission lines associated with neutral oxygen (OI) are identified at wavelengths 630 and 636.6 nm. Furthermore, the spectrum also displays the presence of ionic emission lines of (OII), which are evident at a wavelength of 576.1 nm.

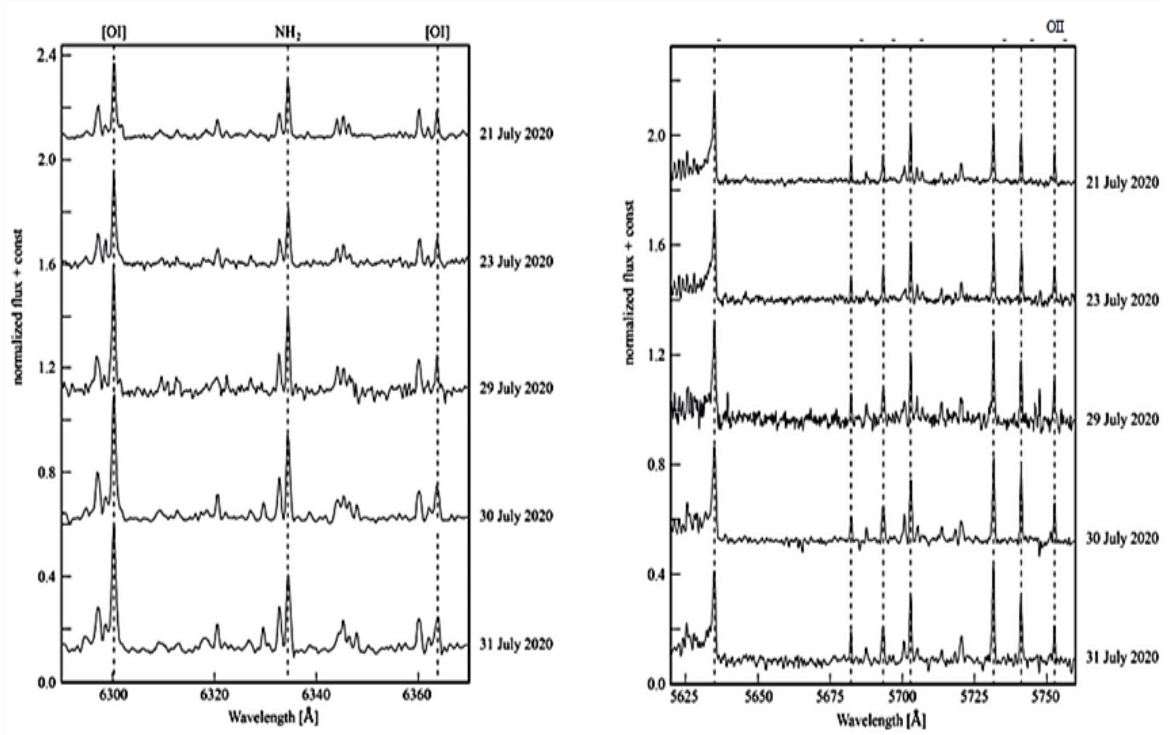

Figure 2: The relation between Intensity (a.u.) and wavelength (nm) for comet C/2020 F3 (NEOWISE).

An additional characteristic involves the presence of neutral NH_2 identifiable at a wavelength of 633.5 nm. Figure 2 illustrates the emission spectrum of oxygen plasma, revealing a greater prevalence of ionic (OII) compared to atomic (OI). Specifically, the emission lines of (OII) with lower intensity at 1.93 a.u. and a wavelength of 576.1 nm were chosen. Similarly, the emission line of (OI) with an intensity of 2.2 a.u. and a wavelength of 636.6 nm was selected, as depicted in Figure 3.

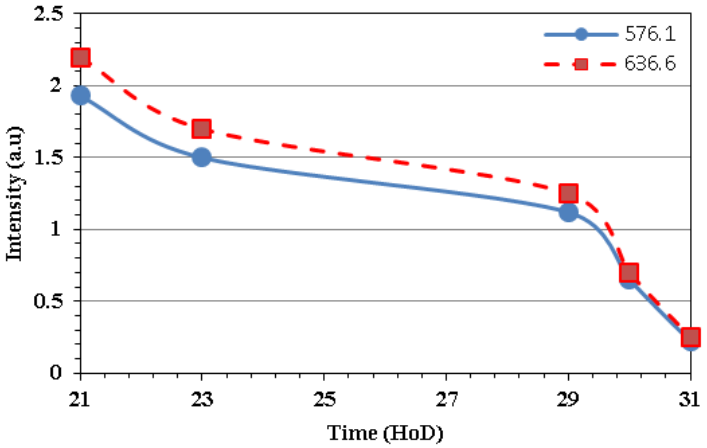

Figure 3: Intensities of the emission spectrum for OI and OII observed during July 21-31, 2020.

These two emission lines were utilized to calculate the plasma parameters of the comet. The necessary physical constants for each emission line were sourced from the atomic spectra database, presented in Table 2, provided by the *National Institute of Standards and Technology* (NIST) [18].

Table 2: The spectroscopic parameters of OI and OII.

Date	Ion	λ (nm)	Intensity (a.u)	g_kA_{ki} (s^{-1})	E_i (eV)	E_k (eV)
21 July 2020	OI	636.6	2.2	3.48e5	46.917	48.865
	OII	576.1	1.93	3.83e6	26.358	28.509
23 July 2020	OI	636.6	1.7	3.48e5	46.917	48.865
	OII	576.1	1.5	3.83e6	26.358	28.509
29 July 2020	OI	636.6	1.25	3.48e5	46.917	48.865
	OII	576.1	1.12	3.83e6	26.358	28.509
30 July 2020	OI	636.6	0.7	3.48e5	46.917	48.865
	OII	576.1	0.65	3.83e6	26.358	28.509
31 July 2020	OI	636.6	0.26	3.48e5	46.917	48.865
	OII	576.1	0.25	3.83e6	26.358	28.509

Based on the analysis of the comet's observed spectrum and the distinct emission lines for each element, the research employed a two-line Ratio Method as its chosen methodology. The two-line Ratio Method was chosen due to the existence of an element with a solitary degree of ionization, as demonstrated in Table 1.

Utilizing the data encompassing wavelengths, intensities, and spectroscopic parameters acquired for comet C/2020 F3 during July 21-31, 2020, calculations of the plasma parameters were performed, including (T_e), (n_e), (λ_D), and (ω_p). The calculated plasma parameter values are presented in Table 3.

Table 3: Calculated plasma parameters for comet C/2020 F3 during 21-31 July 2020

Date	T_e (eV)	n_e (m^{-3})	λ_D (m)	ω_p rad/sec
21 July 2020	0.6087	$3.73x10^{+19}$	$9.50x10^{-07}$	$3.44x10^{+11}$
23 July 2020	0.6072	$3.67\ x10^{+19}$	$9.56\ x10^{-07}$	$3.41x10^{+11}$
29 July 2020	0.6033	$3.53\ x10^{+19}$	$9.72\ x10^{-07}$	$3.35x10^{+11}$
30 July 2020	0.5944	$3.21\ x10^{+19}$	$1.01\ x10^{-06}$	$3.19x10^{+11}$
31 July 2020	0.5767	$2.65\ x10^{+19}$	$1.10\ x10^{-06}$	$2.9x10^{+11}$

Figure 4 illustrates the variations of electron temperature (T_e) and electron density (n_e) within the comet's plasma over the tested time period (Hour of the Day (HoD)). Also, the variation of (λ_D) and (ω_p) for the same period are presented in Figure 5.

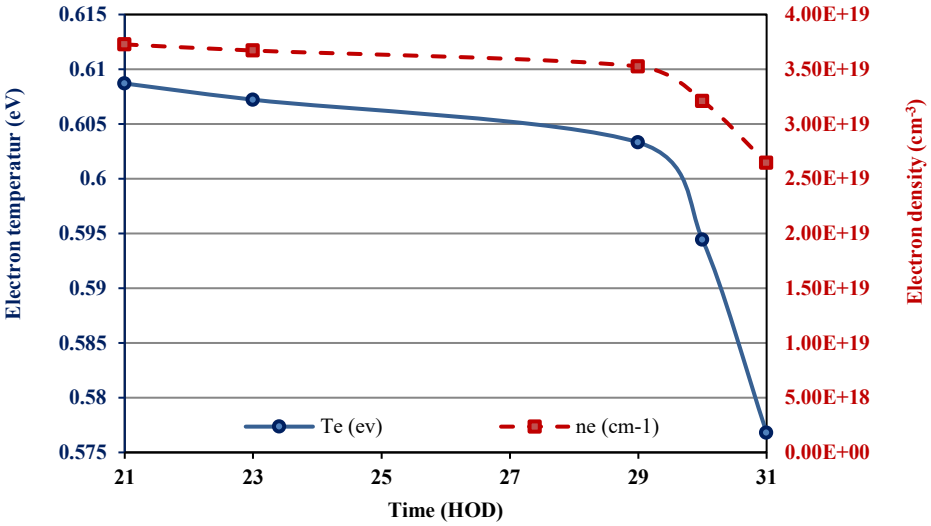

Figure 4: Variations of electron temperature and density during the observation time

From the figure, it can be noticed that as the date progresses within the range of July 21-31, 2020, the electron temperature decreases from 0.6087 eV to 0.576797 eV. Similarly, the electron density decreases from $3.73x10^{+19}$ m^{-3} to 2.65 $x10^{+19}$ m^{-3}, this phenomenon can be attributed to the weakening of ionization processes as the comet moves away from the Sun. This phenomenon can be ascribed to a reduction in the intensity of the lines over time. The electron density of the comet, as indicated in Table 3, is notably elevated.

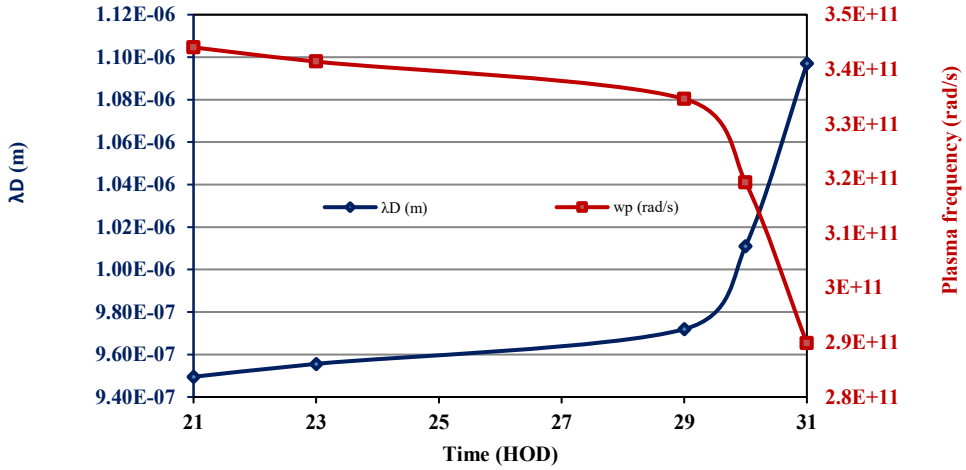

Figure 5: Debye length and plasma frequency vs date, July 2020

This is primarily attributed to the substantial heat carried by the solar wind impacting the comet during its approach from a distance of approximately 0.6040 AU from the Sun. These interactions can result in average temperatures of around 12.2 eV, as reported in [19]. Consequently, the ensuing plasma formed from this interaction is of a considerably high temperature, and the resulting electron density can attain values of up to 2.65 x 10^{19} cm^{-3}, as detailed in [20]. The Debye length represents a distinctive spatial scale defining the separation between ions and electrons within the plasma. The findings showcased in Figure 5, are derived from the current research's investigation of the comet, and they unveil an expansion of the Debye length from $9.50x10^{-07}$ m to $1.10x10^{-06}$ m. This phenomenon arises due to the escalation in electron temperature. Concurrently, the plasma frequency experiences a decrease, transitioning from a magnitude of $3.44x10^{11}$ to $2.9x10^{11}$ rad/sec.

In this paper, the solar wind parameters that are compatible with the comet plasma parameters were also investigated. The plasma parameters of the comet are influenced by the elements of solar wind, as these elements contribute to the formation of plasma in the tail of the comet. The investigated solar wind elements include solar wind temperature (^oK), proton density ($1/cm^3$), solar wind speed (km/s), and magnetic field strength (B_x, B_y, and B_z) in nanoteslas (nT). Figures 6 and 7 depict the variations in the tested solar wind parameters, respectively.

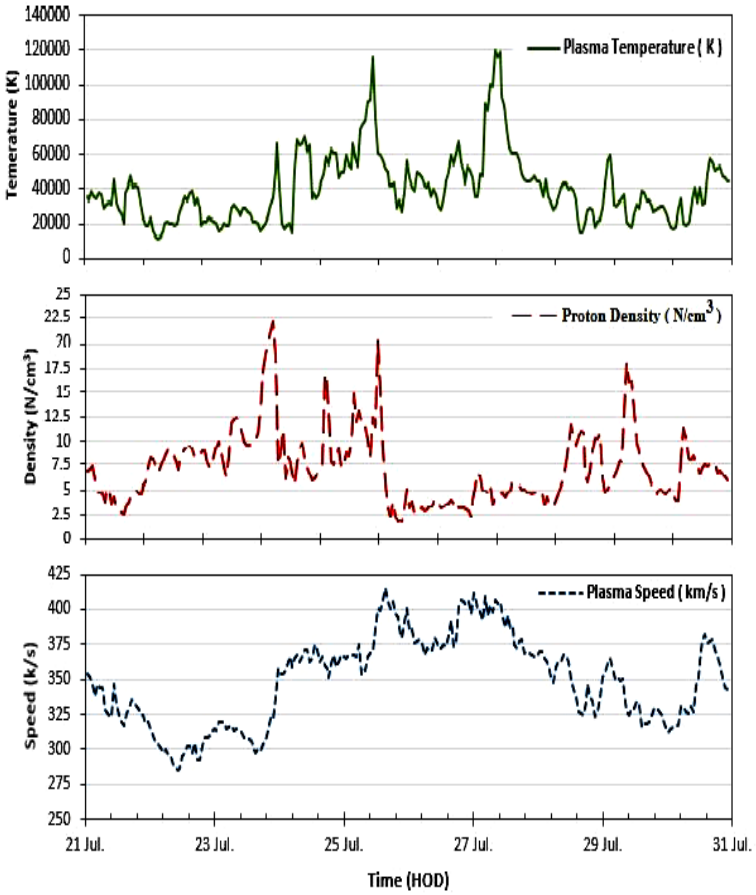

Figure 6: Variations of solar wind temperature, proton density, and solar wind speed during the observation time.

From Figure 6, it can be observed that the solar wind speed and temperature exhibit elevated values in the period 25^{th} to 28^{th} in contrast to the remaining days of the event period. Concurrently, proton density is relatively low during this period. These conditions may influence the temperature and electron density of the plasma. Correspondingly, the plasma parameters of the comet C/2020 F3 exhibit increased values during these specific days, as illustrated in Figure 4. Furthermore, as depicted in Figure 7, it can be noted that the intensity of the magnetic field components (B_y and B_z) showed a more pronounced impact during July (24^{th}-25^{th}) compared to the other days of the event term. In contrast, the B_x component displayed a slight fluctuation throughout the entire study period.

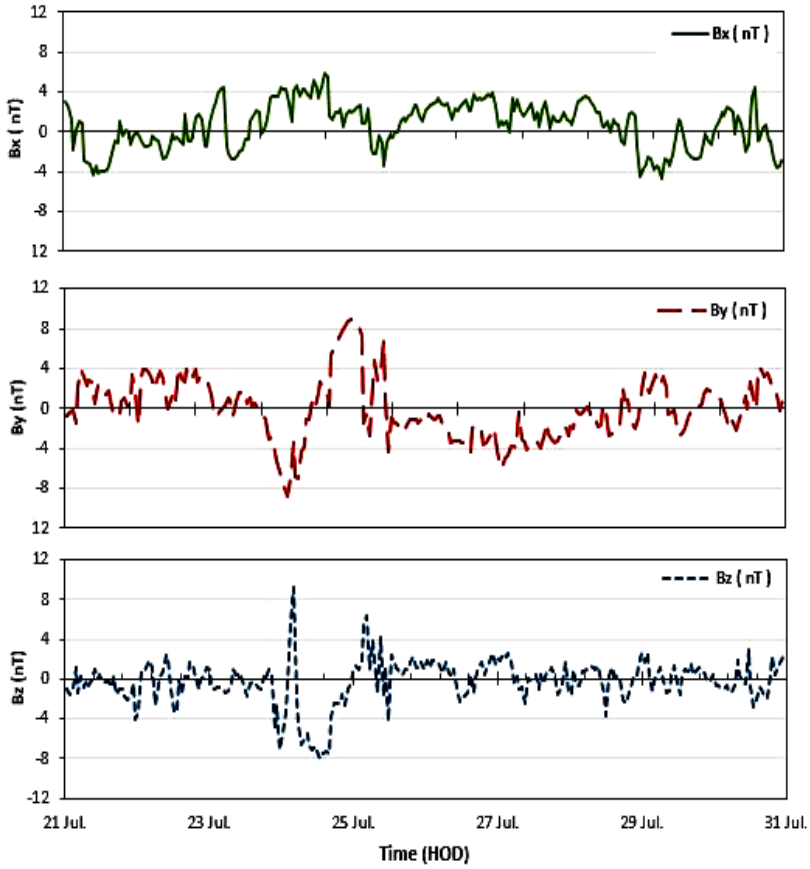

Figure 7: Variations of the solar magnetic field intensity (B_x, B_y, And B_z) during July 21-31, 2020.

6. Conclusions

Based on the preceding findings and discussions, the key conclusions of this study can be summarized as follows: By analyzing the visible and ultraviolet emissions originating from the nuclei of comet C/2020 F3, situated at distances ranging from 0.6040 to 0.8241 astronomical units from July 21 to July 31, 2020, we were able to discern the plasma parameters characterizing this comet. The outcomes of this analysis revealed that the emission line associated with atomic oxygen (OI) displayed the highest intensity, surpassing even the ion (OII) emissions. Notably, the fundamental components constituting the nature of the comet are oxygen (O) and NH_2. Additionally, a significant observation drawn from the electron temperature results indicates a decline in temperature values as the comet moves away from the Sun. This reduction is particularly pronounced during the 30th and 31st days of July. Similarly, electron density follows a similar trend, decreasing as the comet's distance from the Sun increases. During the period spanning from the 25th to the 28th of July, it was observed that solar wind speed and temperature reached elevated values, contrasting with the trends noted during the remaining days of the study. Notably, proton density during this period remained relatively low.

References

[1] Z. Sekanina, "Comet Discovery and Naming," *University of Arizona Press.,* pp. 647-661, 2002.

[2] A. Weaver, "The Reawakening of Cometary Activity in Centaur," *The Astrophysical Journal,* vol. 810, no. 1, p. 833–839, 2015.

[3] P. MANOHARAN, Physics of the Sun and its Atmosphereors, World Scientific, 2008.

[4] K. Mardan and M. and Hadi, "Study the Influence of Solar Activity on the Ionospheric Electron, Ion and Neutral Particle Temperatures over," *Iraqi Journal of Scienc,* pp. 209-217, 2018.

[5] E. D. Trilling, "The Dust Environment of C/2020 F3 (NEOWISE) at One AU," *The Astrophysical Journal Letters,* vol. 898, no. 1, 2020.

[6] P. Cambianica, G. Cremonese, G. Munaretto, C. M. T., M. Fulle, W. Boschin, D. F. L. and .. Harutyunyan, "A high-spectral-resolution catalog of emission lines in the visible spectrum of comet C/2020 F3 (NEOWISE)," *Astronomy & Astrophysics,* vol. 656, no. A160, pp. 1-16, 2021.

[7] L. Cochran Anita, D. Cochran and a. William, "A High Spectral Resolution Atlas of Comet 122P/de Vico," *arXiv:astro,* vol. 38, pp. 1-22, 2020.

[8] M. Knight and K. &. Battams, "Morphology and Photometry of Comet C/2020 F3 (NEOWISE) from SOHO," *ATel,* vol. 13853, 2020.

[9] V. M. Tenishev, "Modeling Plasma and Neutral Gas in Comet C/2013 A1 (Siding Spring) Using a Multifluid Magnetohydrodynamic Approach," *The Astrophysical Journal,* vol. 852, no. 2, p. 110, 2018.

[10] I. Richter, "Rosetta/MIP Ion Measurements at Comet 67P/Churyumov–Gerasimenko," *Space Science Reviews,* vol. 217, no. 1, p. 3, 2021.

[11] M. D. Devia, L. V. Rodriguez-Restrepo and a. E. R. Parra, "Methods employed in optical emission spectroscopy analysis: a review," *Ingeniería y ciencia,* vol. 11, no. 21, pp. 239-267, 2015.

[12] A. M. Waqar, M. S. Rahman, S. Choi, U. Shaislamov, J.-K. Yang, R. Suresh and a. H.-J. Leea, "Measurement of electron temperature and number density and their effects on reactive species formation in a dc underwater capillary discharge," *Applied Science and Convergence Technology,* vol. 26, no. 5, pp. 118-128., 2017.

[13] K. A. Aadim, "Characterization of Laser induced cadmium plasma in air," *Iraqi Journal of Science ,* vol. 56, no. 3B, pp. 2292-2296., 2015.

[14] L. Drogoff, B. J. Margot, M. Chaker, M. Sabsabi, O. Barthelemy, T. W. Johnston, S. Laville, F. Vidal and a. Y. V. Kaenel, "Temporal characterization of femtosecond laser pulses induced plasma for spectrochemical analysis of aluminum alloys," *Spectrochimica acta part B: Atomic spectroscopy ,* vol. 56, no. 6, pp. 987-1002, 2001.

[15] A. A. Kadhim, H. A. AK and a. W. I. Yaseen, "Diagnostics of low-pressure capacitively coupled RF discharge argon plasma," *Iraqi Journal of Physics,* vol. 13, no. 27, pp. 76-82, 2015.

[16] F. Malak Hassan and Y. Waleed Ibrahim, "Electron Density Estimation by Electrostatic Probe for Plasma Generated Near the Spacecraft Returning to the Earth's Atmosphere (2023):," *Iraqi Journal of Science,* pp. 4094-4104, 2023.

[17] H. R. Hamed and A. S. Hussein, "Optical emission spectroscopy for studying the exploding copper wire plasma parameters in distilled water," *Iraqi Journal of Physics,* vol. 15, no. 35, pp. 142-147, 2017.

[18] M. M., G. Avila and a. C. Guirao, "Flechas–a new échelle spectrograph at the university observatory jena," *Astronomische Nachrichten ,* vol. 335, no. 4, pp. 417-427, 2014.

[19] P. W., "20 Jahre Beobachtungsstation Großschwabhausen der Universitäts-Sternwarte Jena," *Jenaer Rundschau ,* vol. 29, no. 3, pp. 121-122, 1984.

[20] B. Richard and a. M. Mugrauer, "Follow-up spectroscopy of comet C/2020 F3 (NEOWISE)," *Astronomische Nachrichten ,* vol. 342, no. 6, pp. 833-839, 2021.

[21] M. M. and a. T. Berthold, "CTK - A new CCD Camera at the University Observatory Jena," *Astronomische Nachrichten: Astronomical Notes,* vol. 331, no. 4, pp. 449-456, 2010.

[22] A. P. Dimmock, K. Nykyri, H. Karimabadi, A. Osmane and a. T. I. Pulkkinen, "A. P. Dimmock, K. Nykyri, H. Karimabadi, AA statistical study into the spatial distribution and dawn□dusk asymmetry of dayside magnetosheath ion temperatures as a function of upstream solar wind conditions," *J. Geophys. Res. Sp. Phys,* vol. 120, p. 2767–2782, 2015.

[23] H. Koskinen, Physics of space storms: From the solar surface to the Earth, Library of Congress Control Number, 2011.

[24] M. Saleh, D. Al-Feadh and a. K. Hadi, "Investigating the correlation of AE-index with different solar wind parameters during strong and severe geomagnetic storms," in *AIP Conference Proceedings*, 2021.

[25] B. Reisenfeld, A. Mewaldt, C. Cummings and a. S. E., "Solar wind radial speed and proton temperature in the inner heliosphere during solar cycle 23. 106(A11),," *Journal of Geophysical Research: Space Physics,* vol. 106, no. A11, pp. 25221-25228., 2001.

[26] T. Gosling, F. Thomsen, J. Bame, T. Feldman and a. G. J., "The solar wind," *Journal of Geophysical Research: Space Physics,* vol. 92, no. A11, pp. 11087-11104, 1987.

[27] S. Esposito, d. Marchetti, R. Ragazzoni and a. A. Baruffolo, " Telescopio Nazionale Galileo," *Space Science Reviews ,* vol. 128, p. 23–66, 2007.

[28] "National Institute of Standards and Technology (NIST) atomic spectra database, (version 5). Available at http://www.nist.gov/pml/data/asd.cfm.".

[29] W. L. B., M. L. Stevens, J. C. Kasper, K. G. Klein, B. A. Maruca, S. D. Bale, T. A. Bowen, M. P. Pulupa and a. C. S. Salem, "The statistical properties of solar wind temperature parameters near 1 AU," *The Astrophysical Journal Supplement Series ,* vol. 236, no. 2, p. 41, 2018.

[30] J. M. Ibrahim, S. Z. Khalaf and a. Q. A. Abbas, "Observation and Theoretical Calculations for Two Comets Plasma Characteristics at Wavelength Range 320-740 nm," in *Conference: second international ConferenceAt: Istanbul- turkey*, Istanbul- turkey, 2021.